



Cite this: *Phys. Chem. Chem. Phys.*,  
2024, 26, 28332

Received 6th October 2024,  
Accepted 26th October 2024

DOI: 10.1039/d4cp03839h

rsc.li/pccp

## Direct capture of the alanine ghost in alanine-doped triglycine sulfate crystals

Yukana Terasawa, <sup>ab</sup> Toshimichi Shibue <sup>c</sup> and Toru Asahi <sup>de</sup>

**In this report, ghostly ultra-trace amounts of alanine in alanine-doped triglycine sulfate crystal were directly observed by solid-state nuclear magnetic resonance, and the presence of two chemical states in the cation form and neutral form in the doped alanine was revealed. As the result, the crystal structure of alanine-doped triglycine sulfate was determined for the first time.**

Doping trace substances into molecular crystals is an important tool for controlling material properties at the molecular level.<sup>1</sup> Triglycine sulfate (TGS)-doped crystals have been extensively studied; the electrical properties of TGS include a low coercive field<sup>2</sup> and high pyroelectricity.<sup>3</sup> TGS has been widely used in infrared spectroscopy and other detection devices because of its high pyroelectricity. To enhance the electrical properties of TGS, various substances have been widely examined, such as TGS doped with EDTA,<sup>4</sup> benzophenone,<sup>5</sup> alanine,<sup>6</sup> and lysine.<sup>7</sup> In particular, alanine-doped triglycine sulfate (ATGS) has been reported to improve the pyroelectricity of TGS<sup>8</sup> and has become the subject of extensive research.

TGS is a crystal composed of glycine and sulfuric acid. In 1956, Matthias *et al.* reported that TGS exhibited ferroelectricity. Generally, ferroelectrics undergo spontaneous polarization ( $P_s$ ) and a phase transition at the Curie temperature  $T_C$ . TGS has spontaneous polarization parallel to the  $b$ -axis and  $T_C$  at 49 °C.<sup>9</sup> TGS belongs to the chiral space group  $P2_1$  and shows ferroelectricity below 49 °C; however, it belongs to the achiral space group  $P2_1/m$  and shows paraelectricity above 49 °C.<sup>10,11</sup> The

crystal structure of TGS was first analyzed using X-ray diffraction by Hoshino *et al.* in 1959, and atomic coordinates other than those of hydrogen were determined.<sup>9</sup> In 1973, Kay *et al.* determined the atomic coordinates of TGS, including hydrogen, by neutron diffraction and analyzed hydrogen bonding in detail.<sup>12</sup> According to the report by Hoshino *et al.*,<sup>9</sup> TGS has the following lattice constants:  $a = 9.15$  (3) Å,  $b = 12.69$  (3) Å,  $c = 5.73$  (3) Å, and  $\beta = 105.7$  (3)°; additionally, it has an asymmetric unit ( $Z = 2$ ) consisting of three crystallographically independent glycines, namely, GI, GII, and GIII, and one sulfuric acid. GI and GIII are in the cation form, and GII is in the zwitterion form.<sup>9,13–16</sup>

The crystal structure of alanine-doped TGS has been studied at the molecular level.<sup>13–15,17–19</sup> Early discussions reported a model in which alanine doping into GI broke the mirror symmetry of the unit cell.<sup>17</sup> On the other hand, Choudhury *et al.* reported that alanine was doped into the zwitterion form GII based on neutron scattering and X-ray diffraction and proposed a model in which the methyl group of alanine doped into GII was a barrier to the inversion of the amino group of glycine in GI.<sup>13–15</sup> Bajpai *et al.* also reported that alanine was doped into GI, followed by molecular reorientation of GII and GIII *via* polarized laser Raman spectroscopy.<sup>18</sup> Thus, many models have been proposed in regard to the doping position of alanine. The difficulty lies in the fact that the amount of doped alanine in the TGS crystals is very low; the alanine doping ratio to TGS ranges from 0.1 to 0.3 mol%.<sup>17,19</sup> As a result, alanine-derived signals cannot be detected by conventional structural analysis because alanine behaves as if it were a ghost in the crystal. To date, no signal derived from doped alanine in crystals has been directly observed, and the position of the doped alanine has been discussed indirectly from the observable TGS signal changes.<sup>13–15,17,18</sup> Meanwhile, ATGS shows extremely unique properties not only in pyroelectricity, but also in ferroelectricity and chirality.<sup>2</sup> It is extremely crucial to determine the crystal structure of ATGS because of its potential for a wide variety of applications.

In this study, L-alanine-doped TGS (LATGS) single crystals were prepared with <sup>15</sup>N-labeled L-alanine, and direct observation

<sup>a</sup> Graduate School of Advanced Science and Engineering, Waseda University, 2-2 Wakamatsu-cho, Shinjuku-ku, Tokyo, 162-8480, Japan

<sup>b</sup> Faculty of Advanced Science and Technology, Kumamoto University, 2-39-1 Chuo-ku, Kurokami, Kumamoto-Shi, Kumamoto, 860-8555, Japan.

E-mail: [terasawa@cs.kumamoto-u.ac.jp](mailto:terasawa@cs.kumamoto-u.ac.jp)

<sup>c</sup> Materials Characterization Central Laboratory, Waseda University, 3-4-1 Okubo, Shinjuku, Tokyo, 165-8555, Japan

<sup>d</sup> Faculty of Science and Engineering, Waseda University, 2-2 Wakamatsu-cho, Shinjuku-ku, Tokyo, 162-8480, Japan

<sup>e</sup> Research Organization for Nano & Life Innovation, Waseda University, 513 Wasedatsurumaki-cho, Shinjuku-ku, Tokyo, 162-0041, Japan



of alanine in the crystal was performed by  $^{15}\text{N}$ -nuclear magnetic resonance (NMR) to determine the doped alanine position and verify the chemical state in the crystal. L-Alanine labeled with  $^{15}\text{N}$  enabled the direct observation of alanine because the  $^{15}\text{N}$  abundance ratio was approximately 300 times greater. Isotropic chemical shifts were measured and analyzed by  $^{15}\text{N}$  magic angle spinning (MAS) NMR, while anisotropic chemical shifts in the single crystals were determined by single-crystal  $^{15}\text{N}$ -NMR. This is the first report on single-crystal  $^{15}\text{N}$ -NMR for analyzing trace amounts of amino acid dopants in molecular crystals; however, this has been reported for peptides using  $^{15}\text{N}$ -labeled amino acids.<sup>20</sup>

A TGS solution was prepared by mixing glycine and sulfuric acid in pure water at a molar ratio of 3:1. For glycine, the weight ratio of  $^{14}\text{N}$ -glycine to  $^{15}\text{N}$ -glycine was approximately 7.7:1. The prepared  $^{15}\text{N}$ -enriched glycine-TGS (TGS; hereafter,  $^{15}\text{N}$ -enriched glycine-TGS is referred to simply as TGS) solution was prepared by solvent evaporation at 20 °C. Moreover, two types of  $^{15}\text{N}$ -L-alanine-TGS (LATGS; hereafter,  $^{15}\text{N}$ -L-alanine-TGS is referred to simply as LATGS) were prepared with a coexistence ratio of  $^{15}\text{N}$ -L-alanine to TGS of 100 mol% and 20 mol% (here,  $^{15}\text{N}$ -L-alanine and  $^{14}\text{N}$ -glycine were used for alanine and glycine of TGS, respectively). The 100 mol% LATGS solution was prepared by mixing  $^{14}\text{N}$ -glycine and sulfuric acid in pure water at a molar ratio of 3:1 and dissolving  $^{15}\text{N}$ -L-alanine at a coexistence ratio of 100 mol% to TGS. The 20 mol% LATGS solution was prepared by diluting the prepared 100 mol% LATGS solution 5-fold with TGS solution. These LATGS solutions were prepared by solvent evaporation at 20 °C.

The as-grown TGS and LATGS crystals were hard and transparent. They exhibited a rhombus-like shape and grew along the crystallographic *b*-axis. The crystal structures were confirmed by single X-ray diffraction analysis. Single-crystal X-ray structure analysis confirmed that both TGS and LATGS had the same structure as previously reported for space group  $P2_1$ ; this consisted of three glycines and one sulfuric acid in an asymmetric unit, but alanine molecules in LATGS were not detected.<sup>2,21</sup> The three glycines are crystallographically independent and defined as shown in Fig. 1.

All  $^{15}\text{N}$ -NMR experiments were performed on a JNM-ECA400 (9.4 T) NMR spectrometer (JEOL, Tokyo, Japan). The resonance frequency of  $^{15}\text{N}$  was 40.5 MHz. The spectral width was 24.3 kHz, and the number of data points was 2048. All spectra

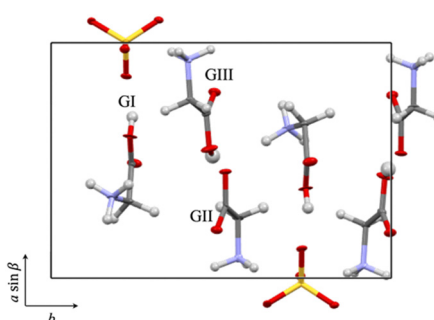


Fig. 1 Crystal structure of TGS. Three crystallographically independent glycines in an asymmetric unit are defined as GI, GII, and GIII.<sup>2,21</sup>

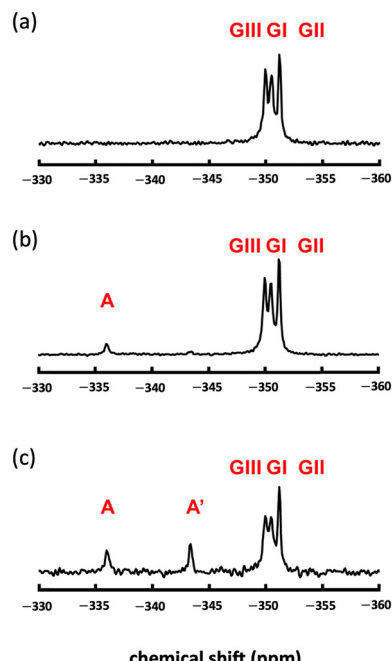


Fig. 2  $^{15}\text{N}$  MAS NMR spectra of (a) TGS, (b) 20 mol% LATGS, and (c) 100 mol% LATGS.

were accumulated to achieve a suitable signal-to-noise ratio. The chemical shifts were calibrated by the external reference ammonium chloride ( $-341.2$  ppm).<sup>22</sup>

The isotropic  $^{15}\text{N}$  chemical shifts of TGS and LATGS were measured by  $^{15}\text{N}$  MAS NMR. TGS and LATGS powders were obtained by grinding single crystals of TGS and LATGS, respectively. The magic-angle spinning rate was 9 kHz, and the repetition time was 5 s. The anisotropic  $^{15}\text{N}$  chemical shift was obtained by single-crystal  $^{15}\text{N}$  NMR.<sup>20</sup> The magnetic field of the NMR is applied perpendicular to the *b*-axis. The single crystal of TGS was rotated by 11.3 degrees, and LATGS was rotated by 22.5 degrees along the magic-angle axis.

Fig. 2a shows the  $^{15}\text{N}$  MAS NMR spectrum of TGS; here, three glycine-derived signals, GI, GII, and GIII, were observed in TGS crystal. These results indicated that  $^{15}\text{N}$  MAS NMR could reveal the differences in the chemical state of the nitrogen in glycine GI, GII, and GIII due to their isotropic chemical shift differences. The observed chemical shifts of the three signals ( $-349.9$  ppm,  $-350.5$  ppm, and  $-351.2$  ppm) were in good agreement with those of glycine observed under sulfate acidity.<sup>23</sup> The chemical shifts of the nitrogen of glycine GI, GII, and GIII in TGS crystals were consistent with the chemical shifts of glycine in TGS crystals, reflecting differences in the hydrogen bonding states formed in TGS crystals, and were observed as differences in the magnetic field shielding from the electrons of the hydrogen nuclei to which the respective nitrogen is directly bound.<sup>24</sup> The average distances between hydrogen and nitrogen atoms determined by neutron scattering were  $1.021$  Å for GI,  $1.017$  Å for GII, and  $1.028$  Å for GIII,<sup>16</sup> and a closer average distance from the hydrogen atom correlated to a greater magnetic field shielding of the nitrogen nucleus. Therefore, the three

TGS signals could be attributed to GI ( $-350.5$  ppm), GII ( $-351.2$  ppm), and GIII ( $-349.9$  ppm).

Fig. 2b shows the  $^{15}\text{N}$  MAS NMR spectrum of 20 mol% LATGS. An alanine-derived signal ( $-336.0$  ppm, as indicated by A in Fig. 2b) was observed independent of the three glycine signals in TGS crystal. The chemical shift at  $-336.0$  ppm was in good agreement with the chemical shift of alanine under acidic conditions.<sup>23</sup> The weight ratio of alanine-derived signal A to glycine in the crystal was 0.147 wt%. The molar ratio of alanine to TGS was 0.12 mol%, which was in good agreement with the doping ratio of alanine obtained from solution circular dichroism spectrum measurements.<sup>21</sup> The alanine-derived signal was observed as a single signal and not three signals, as in the GI to GIII of glycine. Thus, the doping of alanine into GI-GIII was highly selective and occurred at one location among GI-GIII.

Fig. 2c shows the  $^{15}\text{N}$  MAS NMR spectrum of 100 mol% LATGS. In addition to the three glycine signals and the aforementioned alanine-derived signal ( $-336.0$  ppm, as indicated by A in Fig. 2c), a chemical shift ( $-343.4$  ppm, as indicated by A' in Fig. 2c) signal was observed; this was also slightly observed in Fig. 2b. The total weight ratios of alanine-derived signals A and A' to glycine in the crystal were 1.03 wt%. The molar ratio of alanine to TGS was 0.88 mol%, which was in good agreement with the doping ratio of alanine obtained from solution circular dichroism spectrum measurements.<sup>21</sup> This chemical shift ( $-343.4$  ppm) was also an alanine-derived signal; however, instead of a slight difference in hydrogen bonding states (within 1.3 ppm), as in GI-GIII, this difference caused an increased shielding (7.4 ppm), and this increased shielding was likely due to dehydrogenation from alanine nitrogen.<sup>24</sup> The chemical state of this chemical shift ( $-343.4$  ppm) is discussed below; here,  $^{15}\text{N}$  MAS NMR showed the presence of one doping position in TGS and two chemical states in doped alanine.

Here, comparing Fig. 2c with Fig. 2b, the intensity of GI and GIII appears to be slightly decreased due to a broadening of the signal width induced by changing crystallinity with an increase in the doping amount of alanine. As abundance is determined by area rather than intensity in NMR spectra, the area ratios of the GI-, GII-, and GIII-derived signals are nearly identical in 20 mol% LATGS and 100 mol% LATGS, respectively, in Fig. 2.

Also, shown in Fig. 2b and c, with increasing doping amount of alanine, the A' signal is highly sensitive compared to the A signal. This suggests that dehydrogenation from nitrogen in alanine in the crystal is preferential at high alanine doping levels.

Fig. 3a and b show the anisotropic  $^{15}\text{N}$  NMR spectra with the variation of TGS and LATGS single-crystal angles, respectively. The chemical shifts at each angle are summarized in Fig. 3c. The anisotropy of the chemical shifts in the single crystals periodically varies with the orientation of the single crystal relative to the NMR field direction, enabling the analysis of the orientation of the molecules in the crystal.<sup>20</sup> Nitrogen in amino acids such as glycine has the smallest magnetic field shielding tensor along the bound N-C bond axis.<sup>25-27</sup> Therefore, the signal can be attributed to mapping the periodicity of the measured chemical shifts to the orientation of the N-C bond-axes of GI, GII, and GIII in the TGS single crystals.

The periodicity of the glycine-derived signal observed at approximately  $-350$  ppm in the LATGS single crystals is in good agreement with the periodicity of the chemical shifts in the TGS single crystals (Fig. 3c); the glycine molecules GI-GIII in TGS crystals shown in Fig. 1 are from the orientation of the crystal at  $270^\circ$  in Fig. 3c. The N-C bond axes of GII and GIII are oriented along the  $a \sin \beta$ -axis. The magnetic field of the NMR is applied along the  $a \sin \beta$ -axis. The N-C bond axes of GII and GIII are similarly oriented and approximately perpendicular to the N-C bond axes of GI. The N-C bond axes of GII and GIII in Fig. 1 are oriented along the  $a \sin \beta$ -axis direction, which is the direction of the NMR magnetic field. Therefore, the magnetic field shielding of GII and GIII nitrogen at this rotation angle is smaller than that of GI nitrogen, and the chemical shifts are larger for GII and GIII and smaller for GI. As a result, the periodic chemical shifts indicated by the blue squares in Fig. 3c are attributed to GII and GIII, and the periodic chemical shifts indicated by the red circles are attributed to GI. The alanine-derived signal in LATGS single crystals shows a periodicity of chemical shifts similar to that of GI in TGS at lower fields than glycine ( $-330$  to  $-345$  ppm) (Fig. 3c). This result first indicates that alanine is doped into GI in TGS single crystals, and the lack of observed periodicity in the chemical shifts of GII and GIII indicates a high selectivity of alanine doping into GI as well as

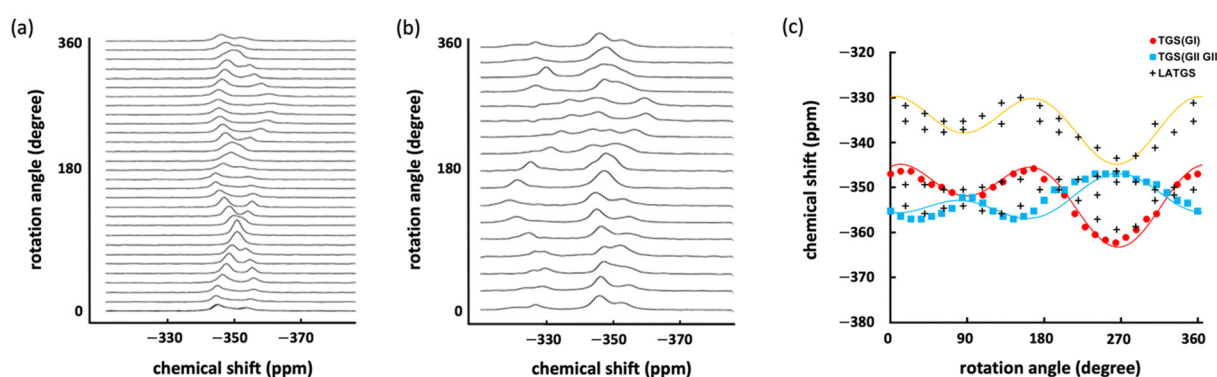


Fig. 3 Single-crystal  $^{15}\text{N}$  NMR of TGS and LATGS. The anisotropic  $^{15}\text{N}$  NMR spectra of (a)  $^{15}\text{N}$ -labeled TGS and (b)  $^{15}\text{N}$ -labeled L-alanine-doped TGS. (c) Anisotropic  $^{15}\text{N}$  chemical shift as a function of single-crystal rotation.



an isotropic spectrum. In addition, two signals derived from alanine doped into GI are observed. Thus, the results obtained from the isotropic and anisotropic  $^{15}\text{N}$  NMR spectra indicate that alanine is highly selectively doped into GI in TGS single crystals and has two different chemical states.

Next, the two chemical states of doped alanine are discussed. In the solution in which the crystals are grown at a pH of 2, the cation and zwitterion of glycine exist in a 2:1 molar ratio, and the ratio in the TGS crystal is also 2:1.<sup>28</sup> Alanine has an isoelectric point similar to that of glycine and a 2:1 molar ratio of cation to zwitterion in solution. Glycine exists in the cation form in GI in TGS crystals. Similarly, the chemical state in which alanine is doped in the cation form in GI is considered signal A ( $-336.0$  ppm) in Fig. 2c. The other chemical state likely originates from the doping of zwitterions in solution; however, as shown in Fig. 2c, the difference in chemical shifts between the cation form (GI, GIII) and the zwitterion form (GII) in TGS is small, within 1.3 ppm, and the chemical states are shifted to higher magnetic fields.

Recent theoretical calculations indicate that zwitterions are stable when two water molecules are hydrogen bonded around alanine; however, the neutral form is stable in the absence of water molecules and is thus susceptible to dehydration.<sup>29,30</sup> Multiple channels are available for proton exchange between the zwitterionic and neutral forms, including the exchange with intramolecular and surrounding water molecules; this results in a minimum energy barrier of  $2.57\text{ kcal mol}^{-1}$ .<sup>31</sup>

The process of incorporating molecules into TGS crystals is described by the Burton–Cabrera–Frank (BCF) surface-diffusion model.<sup>32</sup> The first process is dehydration from the molecules in solution to the adsorbed layer on the crystal surface. During this dehydration, molecules that do not fit into the hydrogen bonding network in the crystal may undergo a conformational change from zwitterionic to neutral since alanine has a low doping ratio and its doping position is limited to GI. Based on these considerations, the following is proposed: alanine in the cation form in the solution is doped into GI in the cation form and is detected as signal A ( $-336.0$  ppm) in Fig. 2c. Additionally, alanine in the zwitterionic form in solution is doped into the neutral form of GI and is detected as signal A' ( $-343.4$  ppm) in Fig. 2c.

## Conclusions

In this study, for the first time,  $^{15}\text{N}$ -labeled L-alanine in TGS crystals was directly observed by  $^{15}\text{N}$ -NMR. Although the doping ratio of alanine to TGS was extremely low, high selectivity for alanine doping into GI in TGS crystals was revealed. Additionally, two chemical states of alanine doped into GI were first reported, and a new model was proposed; in this model, the two chemical states of alanine are as follows: alanine in the cation form in the solution is doped into TGS crystal as the cation form, and alanine in the zwitterion form in the solution is doped into TGS crystal as the neutral form. We finally succeeded in directly capturing the alanine ghost and

determining the crystal structure of ATGS crystal. The  $^{15}\text{N}$ -NMR method with  $^{15}\text{N}$ -labeled L-alanine reported here is not only applicable to  $^{15}\text{N}$ -labeled other amino acid-doped TGS but also expected to be widely applicable to  $^{15}\text{N}$ -labeled nitrogen-containing molecules-doped molecular single crystals.

## Author contributions

The concept for this study was initially drawn by Y. T. TGS and LATGS crystals were grown by Y. T. NMR experiments were conducted by T. S. NMR analysis was performed by Y. T. and T. S. Y. T. and T. S. wrote the manuscript. Y. T., T. S. and T. A. discussed the results at all stages and participated in the development of the manuscript.

## Data availability

Data are available upon request from the authors.

## Conflicts of interest

There are no conflicts to declare.

## Acknowledgements

Y. T. was supported by Mitsubishi Material Research Grant (No. AXA30Z001000) and Waseda University Grants for Special Research Projects (No. BARD00519201, BARD00747301, BARE00772001, BARD01107201). This work utilized the JNM-ECA400, providing MEXT Project for promoting public utilization of advanced research infrastructure (Program for supporting construction of core facilities) Grant Number JPMXS0440500024. All authors express their gratitude to Professor Bart Kahr, New York University for his meaningful advice on NMR experiments.

## Notes and references

1. E. Meirzadeh, I. Azuri, Y. Qi, D. Ehre, A. M. Rappe, M. Lahav, L. Kronik and I. Lubomirsky, *Nat. Commun.*, 2016, **7**, 13351.
2. Y. Terasawa, T. Kikuta, M. Ichiki, S. Sato, K. Ishikawa and T. Asahi, *J. Phys. Chem. Solids*, 2021, **151**, 109890.
3. B. Brezina and F. Smutný, *Czech. J. Phys.*, 1968, **18**, 393–401.
4. K. Meera, A. Claude, R. Muralidharan, C. K. Choi and P. Ramasamy, *J. Cryst. Growth*, 2005, **285**, 358–364.
5. S. Aravazhi, R. Jayavel and C. Subramanian, *Ferroelectrics*, 1997, **200**, 279–286.
6. B. Brezina and M. Havráneková, *Cryst. Res. Technol.*, 1985, **20**, 781–786.
7. R. Parimaladevi, C. Sekar and V. Krishnakumar, *Spectrochim. Acta, Part A*, 2009, **74**, 248–252.
8. P. J. Lock, *Appl. Phys. Lett.*, 1971, **19**, 390–391.
9. S. Hoshino, Y. Okaya and R. Pepinsky, *Phys. Rev.*, 1959, **115**, 323–330.
10. B. T. Matthias, C. E. Miller and J. P. Remeika, *Phys. Rev.*, 1956, **104**, 849–850.



11 E. A. Wood and A. N. Holden, *Acta Crystallogr.*, 1957, **10**, 145–146.

12 M. I. Kay and R. Kleinberg, *Ferroelectrics*, 1973, **5**, 45–52.

13 R. R. Choudhury, R. Chitra, M. Ramanadham and R. Jayavel, *Appl. Phys. A*, 2002, **74**, S1667–S1669.

14 R. R. Choudhury, R. Chitra and M. Ramanadham, *Acta Crystallogr., Sect. B*, 2003, **B59**, 647–652.

15 R. R. Choudhury, R. Chitra, P. U. Sastry, A. Das and M. Ramanadham, *Pramana J. Phys.*, 2004, **63**, 107–115.

16 R. R. Choudhury and R. Chitra, *Pramana J. Phys.*, 2008, **71**, 911–915.

17 E. T. Keve, K. L. Bye, P. W. Whippes and A. D. Annis, *Ferroelectrics*, 1971, **3**, 39–48.

18 P. K. Bajpai and A. L. Verma, *Spectrochim. Acta, Part A*, 2012, **96**, 906–915.

19 M. Koralewski, J. Stankowska and T. Jasinski, *Jpn. J. Appl. Phys.*, 1987, **26**, 383–385.

20 K. W. Waddell, E. Y. Chekmenev and R. J. Wittebort, *J. Am. Chem. Soc.*, 2005, **127**, 9030–9035.

21 Y. Terasawa, T. Kikuta, M. Ichiki, M. Tanaka and T. Asahi, *IEEJ Trans. Sens. Micromach.*, 2022, **142**, 205–213.

22 S. Hayashi and K. Hayamizu, *Bull. Chem. Soc. Jpn.*, 1991, **64**, 688–690.

23 H. R. Kricheldorf, *Magn. Reson. Chem.*, 1979, **12**, 414–417.

24 F. Blomberg, W. Maurer and H. Rueterjans, *Proc. Natl. Acad. Sci. U. S. A.*, 1976, **73**, 1409–1413.

25 C. Gervais, R. Dupree, K. J. Pike, C. Bonhomme, M. Profeta, C. J. Pickard and F. Mauri, *J. Phys. Chem. A*, 2005, **109**, 6960–6969.

26 L. A. O'Dell and R. W. Schurko, *Phys. Chem. Chem. Phys.*, 2009, **11**, 7069–7077.

27 L. A. O'Dell, C. I. Ratcliffe, X. Kong and G. Wu, *J. Phys. Chem. A*, 2012, **116**, 1008–1014.

28 B. Brezina and M. Havráneková, *Cryst. Res. Technol.*, 1985, **20**, 787–794.

29 J. K. Gochhayat, A. Dey and A. K. Pathak, *Chem. Phys. Lett.*, 2019, **716**, 93–101.

30 J. Kim, D. Ahn, S. Park and S. Lee, *RSC Adv.*, 2014, **4**, 16352–16361.

31 A. K. Ojha and S. Bhunia, *J. Mol. Model.*, 2014, **20**, 2124.

32 J. Novotný, F. Moravec and Z. Šolc, *Czech. J. Phys.*, 1973, **23**, 261–272.

